Journal of Thermal Analysis and Calorimetry, Vol. 69 (2002) 205–225

STUDY OF THERMALLY TREATED DICKITE BY INFRARED AND MICRO-RAMAN SPECTROSCOPY USING CURVE-FITTING TECHNIQUE

S. Shoval[1*], *K. H. Michaelian*[2], *M. Boudeulle*[3], *G. Panczer*[3], *I. Lapides*[4] *and S. Yariv*[4]

[1]Geology Group, Department of Natural Sciences, The Open University of Israel, 16 Klausner Street, 61392 Tel Aviv, Israel
[2]Natural Resources Canada, CANMET Western Research Centre, Devon, Alberta, Canada, T9G 1A8
[3]LPCML, UMR 5620 CNRS, Claude Bernard University – Lyon 1, 43 Bd. 11 November 1918, 69622 Villeurbanne Cedex, France
[4]Department of Inorganic and Analytical Chemistry, The Hebrew University of Jerusalem, 91904 Jerusalem, Israel

Abstract

The products of dickite heated in air at 1000 to 1300°C were studied using curve-fitting of transmission and photoacoustic infrared and micro-Raman spectra. The spectra were compared with those of mullite, Al-spinel, corundum, cristobalite, amorphous silica and meta-dickite. Bands that characterize crystalline phases appeared at 1100°C and became stronger with increasing temperature. Mullite, Al-spinel, corundum and amorphous silica were identified by their characteristic bands. The characteristic IR bands of cristobalite overlap those of mullite and amorphous silica, and its presence was therefore established from intensity ratios of the appropriate bands. The research clearly demonstrated the advantage of using curve-fitting for the identification of high temperature phases in the study of the thermal treatment of kaolin-like minerals by infrared and Raman spectroscopy. This technique seems to be a useful method for materials analysis in the ceramic industry.

Keywords: dickite, mullite, spinel, thermal analysis, vibrational spectroscopy

Introduction

The thermal treatment of kaolinite is one of the most important processes in the ceramic industry [1, 2]. It is also carried out in other industries where calcined kaolinite is used as either a pigment or filler [3, 4]. Not surprisingly, the reactions that occur during the heating of kaolinite are widely documented [5–11]. In contrast, there is very little information in the literature about the reactions of dickite during thermal

* Author for correspondence: E-mail: shoval@oumail.openu.ac.il

1418–2874/2002/ $ 5.00

Akadémiai Kiadó, Budapest
Kluwer Academic Publishers, Dordrecht

treatment. Dickite is composed of larger platelets and higher crystallinity and the thermal dehydroxylation occurs at higher temperatures [12, 13].

In a previous publication [14] we described a study of the thermal transformation of dickite by micro-Raman and IR spectroscopy at temperatures from ambient up to 1300°C. That study was preliminary since difficulties arose from the overlap of the bands that were expected to characterize the different thermal products. X-ray peaks of the different thermal products also overlapped and were difficult to interpret. We therefore tried to find a correlation between the recorded vibrational spectra of thermally treated dickite and previous knowledge of the thermal products of kaolinite obtained by different methods.

In the present paper we describe an extension of this earlier study. We concentrate on the vibrational spectra of the reaction products that occur at temperatures 1000–1300°C. In this range high temperature minerals begin to crystallize, whereas at temperatures between 700 and 1000°C most of the material is amorphous to X-rays and is known as meta-dickite. It is expected that the application of curve-fitting techniques to the spectra can lead to identification of the different overlapping components and the determination of the different high temperature phases. In the present work we compare individual bands found in curve-fitted infrared and micro-Raman spectra of thermally treated dickite with those of amorphous silica and meta-dickite and of crystalline mullite Al-spinel, corundum, and cristobalite.

Experimental

Materials

Dickite (the ideal formula $Al_4Si_4O_{10}(OH)_8$) from St. Claire, Pennsylvania, purchased from Wards: Natural Science Establishment, was used in the present study. No impurities were detected in this fraction by powder X-ray diffraction measurements. The IR and Raman spectra of this sample were described previously [15, 16]. Meta-dickite, $Al_4Si_4O_{12}$, was obtained by heating the dickite sample at 700°C for three hours [14]. This temperature was chosen for obtaining the reference since the clay had already been dehydroxylated but the different phases were not yet segregated. Mullite, $3Al_2O_3{\cdot}2SiO_2$, (synthetic, monophasic) was supplied by KPCL (Limoges, France). Cristobalite, SiO_2, was obtained by heating chert (from the Campainian Mishash Formation, Negev, Israel) in an electric kiln for 24 h at 1300°C [17]. The presence of cristobalite was proven by XRD.

Al-spinel (or γ-alumina, γ-Al_2O_3) and corundum, α-Al_2O_3, were obtained by heating boehmite and diaspore, AlOOH, respectively (from flint-clay pisolites, Makhtesh-Ramon, Israel, described in [18]) at 1000°C for three hours. The presence of these phases was shown by XRD [19]. The IR spectrum of the heated boehmite in the range 500–850 cm^{-1} was similar to that of kaolinite heated by Freund at 1000°C in the same range and attributed to Al-spinel [20]. Amorphous silica was purchased from Merck and dried at 300°C.

Methods

Dickite was gradually heated in air to 1300°C in an electric furnace. The heating time at 1000, 1100, 1200 and 1300 was 3 h at each temperature.

Powder X-ray diffractograms were recorded at room temperature with a Philips PW-1710 diffractometer using CuK_{α} radiation.

Micro-Raman spectra were recorded at the different heating temperatures with a Dilor XY confocal micro-Raman spectrometer with a focal length of 500 mm. This instrument is equipped with an Olympus optical microscope, a triple monochromator and a Charge Coupled Device (CCD) EG&G multichannel detector. Spectra were obtained with a 50× objective at a resolution of 3 cm^{-1}. Accumulation times of 360 s were used. The 514.5 nm line of a Spectra Physics 2016 Argon ion laser at a power of 250 mW was used for excitation.

Transmission IR spectra (IR) were recorded at room temperature using a Nicolet FT-IR spectrometer and 'Omnic' software. Disks containing 1 mg of sample in 150 mg of KBr were used. The KBr (IR spectroscopy grade) was supplied by Merck.

Photoacoustic infrared spectra (PA) were obtained at room temperature for non-ground samples at a resolution of either 4 or 6 cm^{-1} using a Bruker IFS 113v spectrometer and a Princeton 6003 PA cell. Spectra were recorded at two different mirror velocities to ensure that no artifacts were included.

The infrared and Raman spectra were analyzed with the Peak fitting function in 'Grams' (Galactic) software. In general Lorentzian shapes were used for the fitting. In very few cases the fitting was improved by using mixed Lorentzian–Gaussian shapes for some of the bands. The curve fitting procedure was based on two principles. All the peaks and shoulders which appeared in the recorded spectrum of the heated dickite were taken into consideration. In addition, data of the spectra of individual reference minerals and the shapes and widths of their bands were introduced by the software for best fit. For the estimation of the total number of peaks, overlapping of neighbour peaks of the different minerals was considered.

Results

X-ray diffraction

X-ray diffractograms of samples heated at 1100–1300°C showed very small peaks due to mullite, γ-alumina and cristobalite. Since these peaks were very weak and appeared on the broad background of an amorphous material, it was difficult to follow the effect of temperature on the intensities of the diffractograms of mullite and cristobalite. However, the diffraction of γ-alumina became very weak with the rise of temperature.

Transmission infrared spectra

All IR spectra which were obtained by transmission spectroscopy, were converted to absorbance spectra. Curve-fitted absorbance IR spectra of the reference materials

mullite, Al-spinel, corundum, meta-dickite, cristobalite and amorphous silica in the range 400–1500 cm^{-1} are shown in Figs 1 and 2. The spectra confirm the results of previous works [21–23]. Frequencies, relative absorbance areas and intensities of the bands are reported in Table 1. Intense bands may be used as fingerprints for the identification of the different thermal products in the spectra of the calcined dickite. These bands are labeled with a 'p' in Table 1.

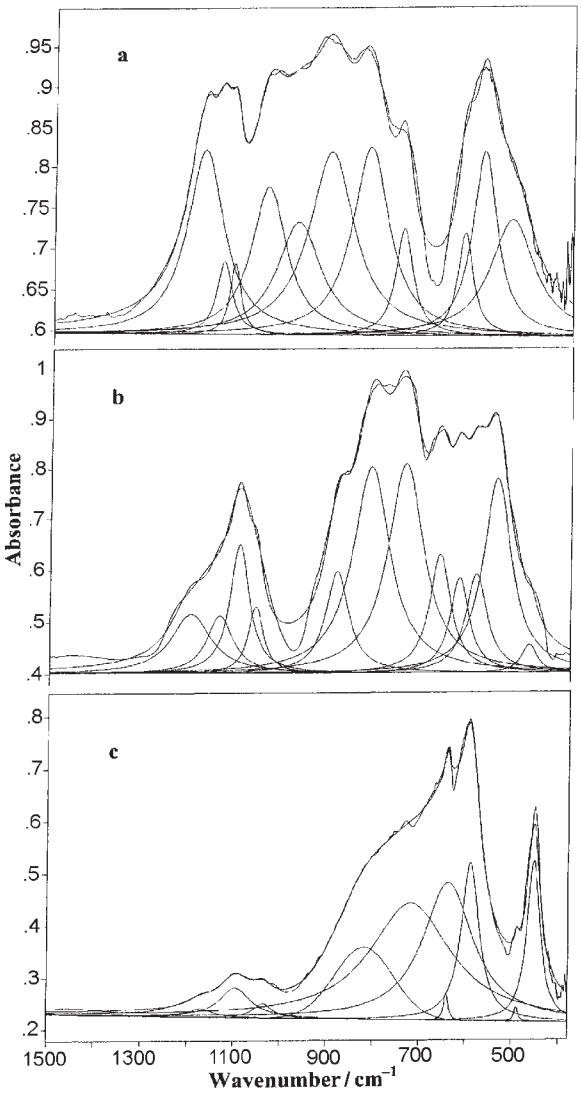

Fig. 1 Curve-fitted transmission IR spectra in the range 400–1500 cm^{-1} of: a – mullite, b – Al-spinel and c – corundum (Chi^2 are 1.88, 5.69 and 1.15, respectively)

Table 1 Frequencies (in cm^{-1}), relative absorbance areas and intensities (in %) of the bands in transmission IR spectra of mullite, Al-spinel, corundum, meta-dickite, cristobalite and amorphous silica obtained by curve-fitting

Assignment	Wave numbers/ cm^{-1}	Relative band area*	Relative intensity**	Assignment	Wave numbers/ cm^{-1}	Relative band area*	Relative intensity**
Mullite a				Meta-dickite b			
SiO_4, AlO_4	1170 p	14.2	97.8		1229	11.0	43.4
	1127 p	2.7	38.5		1160	17.0	63.1
	1103	1.8	37.7	SiO	1104	21.0	100.0
	1031 p	11.1	78.4	SiO	1047	10.0	79.8
SiO_4	965 p	10.6	59.7		896	3.0	24.4
	892 p	17.3	97.0		813	13.0	61.3
AlO_6	807 p	15.0	100.0		707	8.0	29.7
AlO_4	732	4.0	56.7		623	6.0	22.6
	598	3.5	54.5		565	1.0	3.0
AlO_6	556 p	9.7	97.8		472	4.0	40.5
SiO_4	495	10.2	61.5	AlO, SiO	447	6.0	41.7

Table 1 Continued

Assignment	Wave numbers/ cm^{-1}	Relative band area*	Relative intensity**	Assignment	Wave numbers/ cm^{-1}	Relative band area*	Relative intensity**
Al-spinel b				Cristobalite b c			
	1202	6.2	27.9	SiO	1202 p	11.0	27.5
	1140	4.0	27.2		1156	13.0	36.8
	1099	7.0	61.0		1095 p	25.0	100.0
	1064	2.9	31.4		1035 p	24.0	54.2
	892	6.5	47.8		942	4.0	12.8
AlO_6	821 p	20.5	98.5		793	3.0	28.5
AlO_4	748 p	20.1	100.0		754	3.0	9.9
	674 p	7.0	55.6		692	<0.1	4.6
	632 p	4.8	44.6		619 p	1.0	10.6
	596	5.5	46.3		476 p	17.0	66.4
AlO_6	553 p	14.3	92.6				
	484	1.1	13.2				

Table 1 Continued

Assignment	Wave numbers/ cm^{-1}	Relative band area*	Relative intensity**	Assignment	Wave numbers/ cm^{-1}	Relative band area*	Relative intensity **
Corundum d				Amorphous silica b c			
AlO	1095	3.8	18.8	SiO	1220 p	7.5	18.9
	1069	0.8	5.2		1174	14.9	27.3
	1035	1.1	9.0		1100 p	64.9	100.0
	818	12.0	44.6		949	2.3	5.0
	718	34.9	71.0		798	1.7	6.4
	640	0.5	17.4		472 p	8.6	27.2
	637	26.6	85.8				
	589 p	11.5	98.4				
	489	0.2	9.4				
	453	8.4	100.0				

p Band used to characterize the presence of the phase
* Ratio of the area of that band relative to the total band area (in %)
** Ratio of absorbance of that band relative to the most intense band (in %)
Band assignments according to:
a Ruscher [28]
b Freund [20]
c Mishirky *et al.* [22]
d Sato [26]

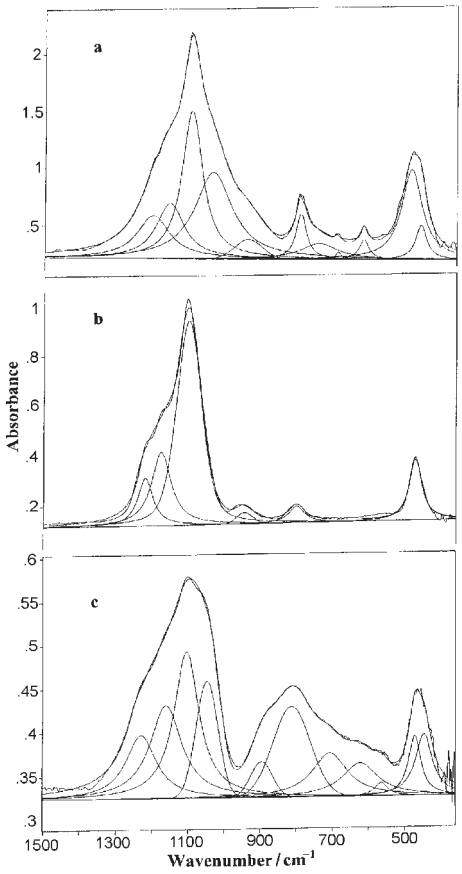

Fig. 2 Curve-fitted transmission IR spectra in the range 400–1500 cm^{-1} of: a – cristobalite, b – amorphous silica and c – meta-dickite (Chi^2 are 1.87, 1.73 and 1.37, respectively)

In a few cases, weak bands can also be used in the identification of the phase that is present. For example, a weak band at 1220 cm^{-1} appears in the spectra of amorphous silica and meta-dickite. No bands appear above 1202 cm^{-1} in the spectra of the crystalline reference minerals. The Si–O–Si group in spectra of pyrosilicates appear above 1100 cm^{-1}. This band shifts to higher frequencies with increasing Si–O–Si angle [24]. Yariv [25] showed that a band at about 1200 cm^{-1} in spectra of phyllosilicates is characteristic for minerals with tetrahedral sheet inversions, such as sepiolite, palygorskite and antigorite. He assigned this band to Si–O–Si groups, which serve as bridges between alternating alumino–Mg–silicate ribbons. An inversion of the tetrahedral sheet requires a Si–O–Si angle of about 180°, which can be stabilized by dπ-pπ bonding in the Si–O–Si group. It appears that a similar type of Si–O

double bond occurs to a small extent in the amorphous silica and the meta-dickite and is responsible for this weak band.

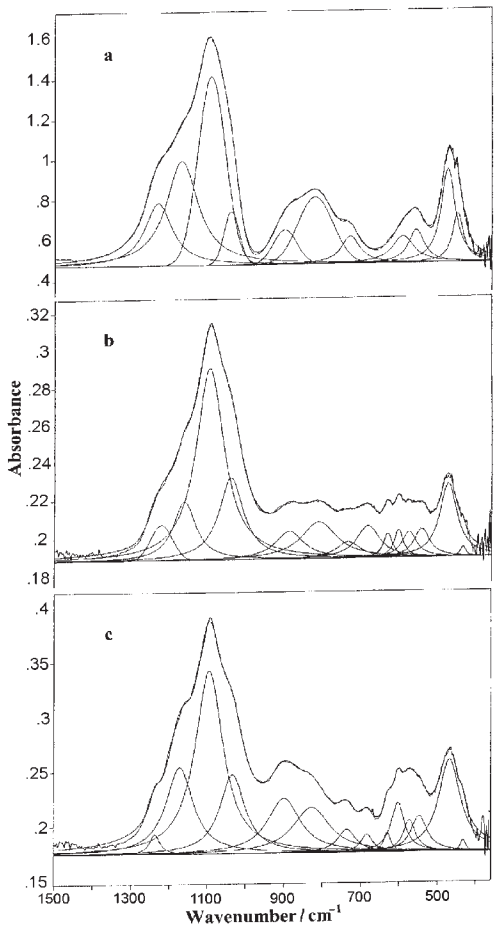

Fig. 3 Curve-fitted transmission IR spectra in the range 400–1500 cm^{-1} of dickite heated at: a – 1000, b – 1100 and c – 1300°C (Chi^2 are 1.33, 0.64 and 0.08, respectively)

Curve-fitted transmission IR spectra of the calcined dickite after heating at 1000, 1100 and 1300°C are shown in Fig. 3. Frequencies, relative absorbance areas and intensities of the bands (including those of a sample heated at 1200°C) are given in Table 2. The different phases that are represented by these bands are also given in the Table. All of these fitted spectra show a weak band at 1221–1237 cm^{-1} that implies the presence of amorphous silica and/or meta-dickite. The relative area of this

Table 2 Frequencies (in cm^{-1}), relative absorbance areas and intensities (in %) of the bands in transmission IR spectra of thermal products of dickite heated at 1000, 1100, 1200 and 1300°C obtained by curve-fitting

Phase	Wave numbers/ cm^{-1}	Relative band area*	Relative intensity**	Phase	Wave numbers/ cm^{-1}	Relative band area*	Relative intensity**
	Calcined dickite 1000°C				Calcined dickite 1200°C		
A, D	1232	11.4	32.6	A	1232	0.8	8.3
A, D	1170	22.3	55.2	M	1171	10.4	39.8
A, D	1092	24.6	100.0	A, C	1097	29.9	100.0
D	1040	3.8	27.9	C, M	1038	16.9	57.1
D	900	3.8	8.0	M	899	7.8	25.0
D	821	10.9	35.0	M, C	830	9.1	23.2
D	729	3.5	14.2	M, S	738	2.6	11.9
				S	687	2.6	15.5
				S	629	1.3	16.1
					602	2.6	20.8
Cor	592	3.8	13.9	Cor	573	3.9	25.6
D	557	3.5	17.1	M, S	543	3.9	22.6
A, D	474	8.8	49.2	A, C	470	7.8	45.8
	449	3.5	25.7		452	0.6	9.5

Table 2 Continued

Phase	Wave numbers/ cm^{-1}	Relative band area*	Relative intensity**	Phase	Wave numbers/ cm^{-1}	Relative band area*	Relative intensity**
	Calcined dickite 1100°C				Calcined dickite 1300°C		
A	1221	3.6	19.0	A	1237	1.2	10.7
M	1161	8.8	31.0	M	1172	13.3	47.3
A, C	1095	35.6	100.0	A, C	1095	29.2	100.0
C, M	1040	13.4	43.0	C, M	1034	11.4	43.1
M	888	5.3	15.0	M	898	10.1	29.9
M, S	811	8.5	19.0	M, S	829	9.4	25.1
M, S	734	2.6	9.0	S	737	2.4	12.6
S	682	4.9	20.0	S	681	1.2	9.6
S	630	1.5	13.0	S	626	2.0	10.8
	602	1.7	15.0		603	3.8	26.9
Cor	575	2.5	13.0	Cor	577	2.2	17.4
M, S	541	2.9	15.0	M, S	550	3.2	19.2
A, C	473	8.1	39.0	A, C	467	10.5	49.7
	434	0.3	5.0		434	0.3	6.6

A – Amorphous silica; C – Cristobalite; D – Meta-dickite; M – Mullite; S – Al-spinel; Cor – Corundum
* Ratio of the area of that band relative to the total band area (in %)
** Ratio of absorbance of that band relative to the most intense band (in %)

band decreases with the increase in temperature, indicating that the amorphous phases are transformed into crystalline phases.

The four spectra show a weak band at 1161–1172 cm^{-1}. This band corresponds to the principal band in the spectrum of mullite. Cristobalite, meta-dickite and amorphous silica also contribute to this absorption. The relative intensity of this band is very high in the spectrum of the sample heated at 1000°C. It decreases at 1100°C and increases again at 1200 and 1300°C. We suggest that at 1000°C it represents residual meta-dickite and amorphous silica, and at higher temperatures, mullite.

The ratio between the areas of the 1230 and the 1170 cm^{-1} bands is 0.65, 0.50, 0.51, 0.41, 0.08 and 0.09 in the spectra of meta-dickite and amorphous silica and of dickite heated at 1000, 1100, 1200, and 1300°C, respectively. These results are in agreement with the fact that the content of meta-dickite decreases and that of mullite increases with the rise in temperature. Since mullite is formed only above 1000°C, the decrease of these ratios in the dickite heated at 700 to 1000°C indicates that some amorphous silica is segregated at this temperature interval, as suggested by Freund [20].

The presence of mullite in the samples heated at 1100–1300°C is confirmed by the appearance of an intense band at 888–900 cm^{-1}. This band gradually intensifies when the sample is heated to 1300°C. The relative area of this band is very small in the spectra of meta-dickite and dickite treated at 1000°C. Therefore it may be concluded that mullite crystallizes only above 1000°C and its content increases with the rise in temperature. The shift of the characteristic bands with the temperature increase may indicate solid-state changes during the thermal treatment.

The bands at 1170 and 892 cm^{-1} in the spectrum of neat mullite have relative intensities of 97.8 and 97.0% and may therefore be used to determine the changes in the content of this mineral with increasing temperature. The other crystalline phases show only weak absorption in these locations that can be ignored for semi-quantitative estimation. Table 2 shows that these bands are intensified with the increase in temperature from 1100 to 1300°C, indicating that the content of mullite increases with the increase in temperature.

The spectra of the thermally treated dickite show a very intense band at 1095 cm^{-1} and another weaker band at 475 cm^{-1}. The combination of these two bands appears in the spectra of cristobalite and amorphous silica. The ratio between the absorbance areas of the 1100 and the 475 cm^{-1} bands is 2.1, 1.5, 7.5, 2.0, 4.4, 3.6 and 2.8 in the spectra of meta-dickite, cristobalite and amorphous silica, and of dickite heated at 1000, 1100, 1200 and 1300°C, respectively. This indicates that the sample heated at 1000°C contains residual meta-dickite. The samples heated above 1000°C contain cristobalite as well as amorphous silica. This also shows that the amount of the amorphous phase decreases as temperature increases. A very weak band at 1103 cm^{-1} appears in the spectrum of mullite. This band is very weak in comparison to the feature in the spectra of cristobalite and amorphous silica and can be ignored in this case.

A band occurs at 1031–1035 cm^{-1} in the spectra of cristobalite and mullite. The ratio between the areas of the 1100 and 1035 cm^{-1} bands in the spectra of cristobalite and mullite are 1.04 and 0.16, respectively. These two bands have the highest relative band areas in the cristobalite spectrum. In the spectra of dickite heated at 1000, 1100,

1200 and 1300°C, this ratio equals 6.5, 2.6, 1.7 and 2.5, respectively. This is also due to the fact that the 1100 cm^{-1} band is common to cristobalite, mullite and amorphous silica. The significant change in the ratio between 1000 and 1100°C supports the idea that cristobalite and mullite crystallized above 1000°C.

Bands at 553, 748 and 821 cm^{-1} are very intense in the spectrum of Al-spinel. The 748 cm^{-1} band is characteristic for AlO_4 [26, 27]. Weaker bands of this mineral appear at 632, 674, 892 and 1099 cm^{-1}. The bands at 632 and 674 cm^{-1} in the spectra of calcined dickite may be used to identify the presence of Al-spinel. These features, although not the most intense bands of this mineral, appear in a region where there are no absorption bands of cristobalite, mullite or amorphous silica. These two bands do not appear in the fitted spectrum of dickite heated at 1000°C. The intense band at 821 cm^{-1} is already observed at this temperature and two weak bands at 557 and 729 cm^{-1} probably represent residual meta-dickite. According to Gualtieri and Bellotto [10], in the calcination of kaolinite the thermal transformation from meta-kaolinite to mullite goes through a short-range ordered material. A similar material may be obtained during the calcination of dickite. This could have the Al-spinel structure. According to Sato [26] a band at 681 cm^{-1} represents Al located in tetrahedral sites. The band that is detected at 682 cm^{-1} in the curve-fitted spectrum of dickite heated at 1100°C may indicate this feature. This band, which was not observed in samples heated at lower temperatures (e.g. 1000°C), persisted at higher temperatures but became very weak. The weakening of the band confirms the work of Gualtieri and Bellotto [10], who stated that the Al-spinel is transformed into mullite. The bands at 632 and 682 cm^{-1} and their relative intensities drastically decrease by heating the sample from 1100 to 1300°C. This indicates that the content of Al-spinel decreases during this thermal treatment. An increase in the intensities of the mullite bands and a decrease of the amorphous silica bands also accompany the treatment. It appears that during this heating the amorphous silica reacts with Al-spinel and mullite is formed.

A weak band at 592 cm^{-1} appears at 1000°C. This band shifts to 575 cm^{-1} at 1100°C and persists at higher temperatures. This observation suggests that a very small amount of corundum is obtained during the thermal treatment [26]. It should be noted that the presence of minor amounts of corundum was detected through luminescence spectroscopy by the appearance of the R-lines of Cr^{3+} impurity at 692 and 694 nm in our previous study [14].

Photoacoustic (PA) IR spectra

The entire mid-infrared PA spectra of dickite heated at 1100 and 1300°C are displayed in Fig. 4. It is especially interesting to note the appearance of a series of bands above 1300 cm^{-1} in these spectra. There are three small bands at 1300–2000 cm^{-1} in the spectrum of the sample heated at 1100; these intensify considerably in the sample heated at 1300°C. In the spectral range 1400–2500 cm^{-1} of the latter sample, well-defined bands are observed at 1436, 1624, 1762, 1877, 2000 and 2285 cm^{-1}. These features are due to overtones and combinations of the less well resolved bands

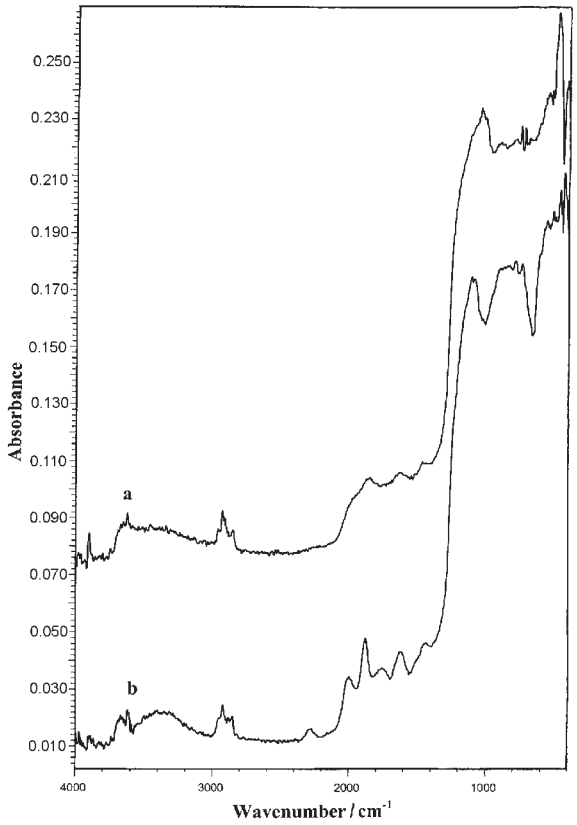

Fig. 4 Photoacoustic IR spectra in the range 400–4000 cm^{-1} of dickite heated at: a – 1100 and b – 1300°C

at lower frequencies, which were discerned by the curve-fitting calculations. These bands were not observed in any of the spectra recorded by the transmittance infrared.

Curve-fitted PA spectra in the range 400–1500 cm^{-1} of calcined dickite heated at 1100 and 1300°C are shown in Fig. 5. Frequencies, relative absorption areas and intensities of the bands are gathered in Table 3. The relative areas and intensities of the bands depend on the presence of crystalline phases, which are controlled by the heating temperature. In the curve fitted spectrum of dickite heated at 1300°C most of the bands are more intense than the correlative bands in the sample heated at 1100°C. Specifically, the relative areas of the crystalline phases increased with temperature. In these samples there is satisfactory correlation between the PA and the transmittance IR spectra in the relative areas of the correlative bands of each heating temperature (compare the changes in the relative band areas in Tables 2 and 3). For example, the relative areas of bands at 1182 and 1012 cm^{-1}, which characterize mullite and cristobalite, respectively, increase with a rise in temperature, whereas those of the bands at 691 and 625 cm^{-1}, which characterize Al-spinel, decrease with the rise in temperature. This is also the case with the principal band of amorphous silica at

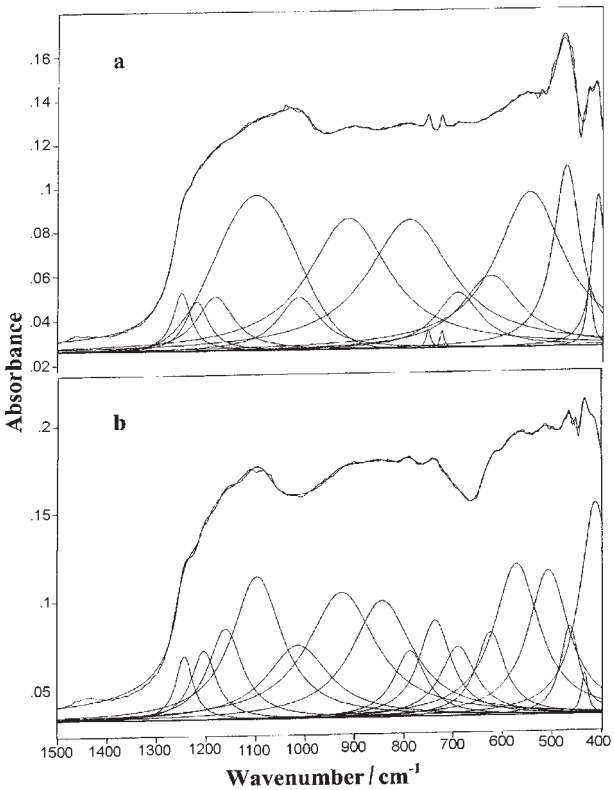

Fig. 5 Curve-fitted photoacoustic IR spectra in the range 400–1500 cm^{-1} of dickite heated at: a – 1100 and b – 1300°C (Chi^2 are 0.67 and 1.44, respectively)

1100 cm^{-1}, which decreased with a rise in temperature. It should be mentioned that most other bands of amorphous silica characterize other minerals as well.

Micro-Raman spectra

Curve-fitted micro-Raman spectra in the range 200–620 cm^{-1} of mullite, corundum and amorphous silica are shown in Fig. 6. These spectra confirm the results of previous works [28–30]. The diagnostic peaks are collected in Table 4. In addition to the IR bands, these may be used as fingerprints for the identification of the different thermal products in the micro-Raman spectra of calcined dickite and other kaolin-like minerals. Curve-fitted spectra of the thermally treated dickite samples in this range are shown in Fig. 7. These spectra show a very weak band at 606 and a more intense band at 487 cm^{-1} known as D_2 and D_1 bands in the Raman spectrum of amorphous silica [31]. It should be noted that the weak 606 cm^{-1} band also appears in the spectrum of mullite and therefore should not be considered diagnostic for amorphous silica. A band at 443–455 cm^{-1} in the spectra of calcined dickite is also characteristic of amorphous silica.

Table 3 Frequencies (in cm^{-1}), relative absorbance areas and intensities (in %) of the bands in photoacoustic IR spectra of thermal products of dickite heated at 1100 and 1300°C obtained by curve-fitting

Wave numbers/ cm^{-1}	Relative band area*	Relative intensity**	Wave numbers/ cm^{-1}	Relative band area*	Relative intensity**
Calcined dickite 1100°C			Calcined dickite 1300°C		
1250	2.0	31.7	1244	1.9	39.0
1220	2.1	26.8	1204	2.9	41.3
1182	3.6	29.3	1162	5.1	54.6
1100	16.1	85.3	1098	11.6	84.1
1012	4.0	29.3	1019	6.8	40.3
912	17.9	71.9	927	15.2	76.9
			838	13.1	73.6
790	18.0	71.0	785	2.8	33.6
751	0.1	9.8	739	3.5	45.4
723	0.1	9.8			
691	4.3	30.5	699	3.5	38.0
625	7.2	39.0	620	6.5	54.7
			579	0.3	6.8
546	16.3	85.4	546	16.1	100.0
472	8.0	100.0	463	9.8	91.0
433	0.3	6.8	433	0.3	6.8

* Ratio of the area of that band relative to the total band area (in %)
** Ratio of absorbance of that band relative to the most intense band (in %)

Table 4 The most intense bands in the micro-Raman spectra of mullite, Al-spinel, corundum, meta-dickite, cristobalite and amorphous silica obtained by curve-fitting

Material	Wave numbers/cm^{-1}	Material	Wave numbers/cm^{-1}
Mullite		Mg–Al-spinel	407 vs
	1135 vw		
	1126 vw	corundum	417 vs
	1034 w		
	961 vs	cristobalite	408 vs
	607 vw		226 vs
	413 vs		
	338 m	amorphous silica	606 vw
	308 s		487 s
			429 vs, vb

w– weak; *m* – medium; *s* – strong; *v* – very; *b* – broad

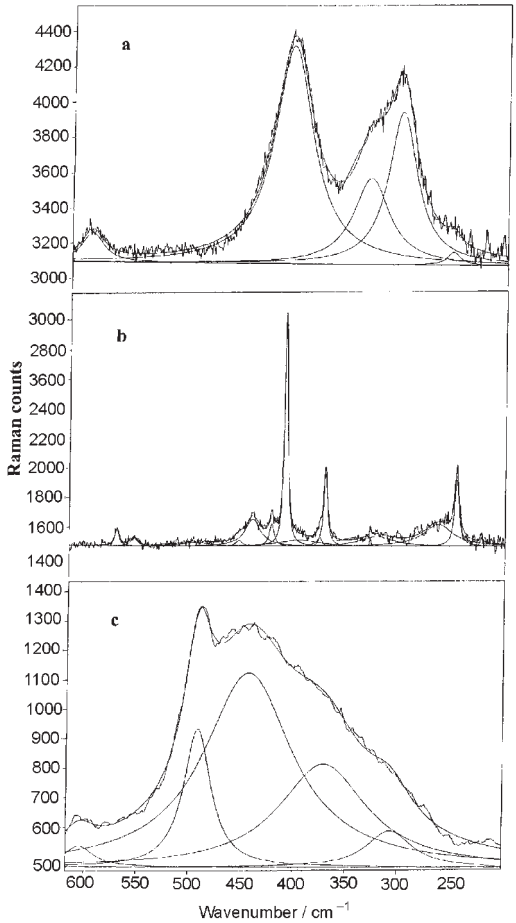

Fig. 6 Curve-fitted micro-Raman spectra in the range 200–620 cm^{-1} of: a – mullite, b – corundum and c – amorphous silica (Chi^2 are 1.73, 2.45 and 5.61, respectively)

At 1200 and 1300°C characteristic bands of mullite at 308, 338 and 413 (very intense) cm^{-1} appear, proving the presence of this mineral. Bands at 294, 341 and 422 cm^{-1}, which are observed in the curve-fitted spectrum of the sample heated at 1100°C, are weak and may be considered as belonging to a mullite precursor.

The micro-Raman spectrum of corundum has a diagnostic band at 417 cm^{-1}. It should be mentioned that very small amounts of corundum were detected from the transmittance IR spectra. It was impossible to identify this band in some of the micro-Raman spectra of the calcined dickite because it overlaps a mullite band. However, in several micro-Raman spectra corundum was clearly observed. The lack of homogeneity of the sample is due to the fact that it had not been ground before the micro-Raman spectrum was recorded. It should be noted that for micro-Raman spectroscopy measurements, unground samples are to be used.

Cristobalite exhibits two strong Raman bands at 226 and 408 cm^{-1} (Table 4). The feature at 408 cm^{-1} may overlap the mullite band, but the band at 226 cm^{-1} is diagnostic. This band was not observed in the examined micro-Raman spectra of thermally treated dickite. It should be noted that cristobalite was identified from the transmission IR spectra of the thermally treated samples, which showed that its content increased with temperature. Since the sample for the micro-Raman study lacks homogeneity, it is possible that we were unsuccessful in directing the laser beam on a crystal of cristobalite.

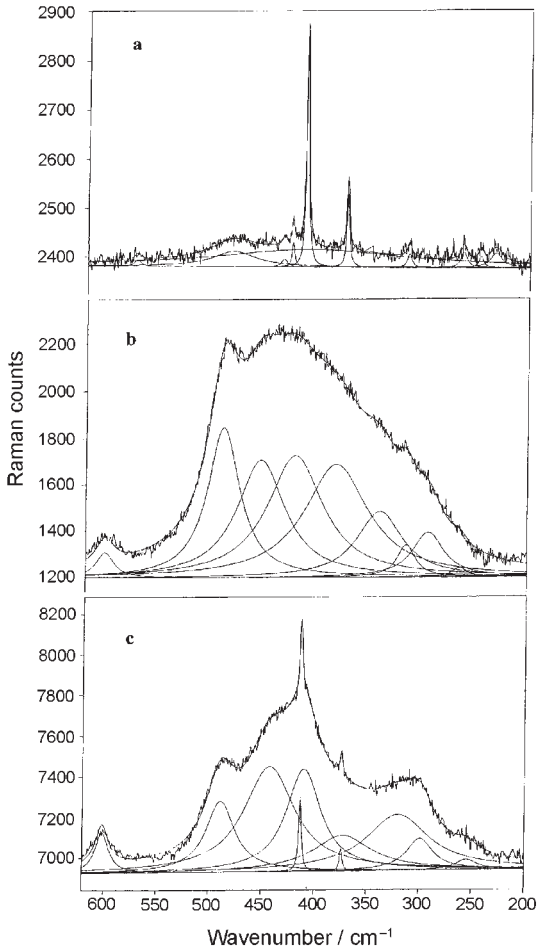

Fig. 7 Curve-fitted micro-Raman spectra in the range 200–620 cm^{-1} of calcined dickite heated at: a – 1000, b – 1100 and c – 1300°C (Chi^2 are 0.48, 1.71 and 0.61, respectively)

Discussion

The use of vibrational spectroscopy in the study of the thermal transformations of clay minerals and ceramic materials is limited by the fact that the characteristic absorptions of the different thermal products have very similar locations such that bands of different phases overlap [32]. Based on infrared spectra of kaolinite heated from 30 to 1200°C, Freund [20] described the structure of meta-kaolinite and its reaction sequence Si–Al-spinel to mullite through thermal transformation. The spectra show very broad absorptions with broad maxima and shoulders and in fact, Freund's conclusions were based on shifts and splitting of these maxima or shoulders. In the present study, we demonstrate that in the curve-fitting technique the characteristic spectra of the different thermal products are clearly obtained and specific bands that characterize the different phases can be elucidated.

This research has clearly demonstrated the advantage of using curve-fitting for the identification of high temperature phases in the study of the thermal treatment of kaolin-like minerals by infrared and Raman spectroscopy. Dickite was thermally treated in this work. The present results, and those of previous study [12–14], showed that this mineral undergoes thermal reactions similar to those of kaolinite. In the first stage the clay is dehydroxylated and transformed to meta-dickite. This reaction, which already occurs at about 510°C in kaolinite [20, 33], takes place only at 700°C in dickite [12].

The meta-phase, which is amorphous to X-rays in the dehydroxylated phase of kaolinite, also responds similarly in the dehydroxylated phase of dickite. New crystalline phases begin to appear only above 1000°C, and their content increases concomitantly with temperature. However at 1300°C, a great part of the material is still amorphous to X-rays.

In our previous study we showed that the Raman spectra of dickite treated at temperatures between 700 and 1000°C do not display any bands. However, the Raman spectra become more significant above 1000°C. The present curve-fitting study showed that only three phases were identified by this technique, namely mullite, corundum and amorphous silica which was expelled from the meta-dickite.

Infrared spectra are sensitive to the chemical bonds and the symmetry of the solid phase. At temperatures between 700 and 1000°C the infrared spectra showed bands characteristic of meta-dickite. Bands that arise from the crystalline phases appeared at 1100°C and became stronger with increasing temperature. Mullite, Al-spinel and corundum were positively identified by their characteristic bands. Cristobalite was also identified, but some of its bands overlap those of amorphous silica, and its presence was therefore established from intensity ratios of the bands.

Conclusions

In the present study we show that the curve-fitting of infrared and micro-Raman spectra of thermal products of dickite enables direct identification of the different phases that occur in the mixture. Vibrational spectroscopy enables identification of changes

in the amorphous and crystalline ceramic materials, whereas X-ray diffraction is limited to examination of crystallized materials. It is concluded that the former technique is a useful method for materials analysis in the ceramic industry.

* * *

We gratefully acknowledge the support of the Open University of Israel Research Fund and the CNRS/INSU (Geomatériaux Program), France.

References

1 D. Arnold, Ceramic theory and cultural process. Cambridge University Press, Cambridge 1985.
2 R. R. West, in 'Differential Thermal Analysis' (R. C. Mackenzie, Ed.) Academic Press, London 1972, Vol. 2, p. 149.
3 P. Sennet, in 'Kirk-Othner Encyclopedia of Chemical Technology', 4th edition, Wiley, New York 1992, Vol. 6, p. 405.
4 H. H. Murray, in 'Ullman's Encyclopedia of Industrial Chemistry', 5th edition, VCH, Berlin 1985, Vol. A7, p. 109.
5 M. Belloto, A. Gualtieri, G. Artioli and S. M. Clark, Phys. Chem. Miner., 22 (1995) 207.
6 D. Massiot, P. Dion, J. F. Alcover and F. Bergaya, J. Amer. Ceram. Soc., 78 (1995) 2940.
7 J. Dubois, M. Murat, A. Amroune, X. Carbonneau and R. Gardon, Appl. Clay Sci., 10 (1995) 187.
8 P. Dion, J.-F. Alcover, C. Clinard and D. Tchoubar, J. Mater. Sci., 31 (1996) 5069.
9 P. Dion, J.-F. Alcover, F. Bergaya, A. Ortega, P. L. Llewellyn and F. Rouquerol, Clay Miner., 33 (1998) 269.
10 A. Gualtieri and M. Bellotto, Phys. Chem. Miner., 25 (1998) 442.
11 M. P. Riccardi, B. Messiga and P. Duminuco, Appl. Clay Sci., 15 (1999) 393.
12 L. Stoch, J. Thermal Anal., 29 (1984) 919.
13 R. L. Frost and A. M. Vassallo, Clays Clay Miner., 44 (1996) 635.
14 S. Shoval, M. Boudeulle, S. Yariv, I. Lapides and G. Panczer, Optic. Mater., 16 (2001) 319.
15 C. T. Johnston, J. Helsen, R. A. Schoonheydt, D. L. Bish and S. F. Angew, Amer. Miner., 83 (1998) 75.
16 S. Shoval, S. Yariv, K. H. Michaelian, M. Boudeulle and G. Panczer, Clays Clay Miner., 49 (2001) 347.
17 S. Shoval, B. Champagnon and G. Panczer, J. Thermal Anal., 50 (1997) 203.
18 S. Shoval, S. Yariv, M. Boudeulle and G. Panczer, in 'Clays for our future' (H. Kodama, A. R. Mermut & J. K. Torrance, eds.), ICC 1997, Ottawa, Canada 1999, p. 623.
19 S. Shoval, B. Champagnon, G. Panczer, M. Gaft and M. Boudeulle, Proc., Semaine Franco-Israelienne, Université Claude Bernard, Lyon, France 1999.
20 F. Freund, in 'The infrared spectra of minerals' (V. C. Farmer ed.), Mineralogical Society, London 1974, p. 465.
21 H. H. W. Moenke, in 'The infrared spectra of minerals' (V. C. Farmer ed.), Mineralogical Society, London 1974, p. 365.
22 S. Mishirky, S. Yariv and Siniarsky, Clay Sci., 4 (1974) 213.
23 H. W. Van der Marel and H. Beutelspacher, 'Atlas of infrared spectroscopy of clay minerals and their admixtures'. Elsevier 1976.

24 A. N. Lazarev, in 'The Infrared Spectra of Minerals' (V. C. Farmers ed.) Mineralogical Society, London 1974, p. 69.
25 S. Yariv, Clay Miner., 21 (1986) 925.
26 T. Sato, 'Preparation of aluminium hydroxides and aluminas', Litarvan Literature, Nedherland, Colorado 1996.
27 S. M. Bradley, R. A. Kydd and R. F. Howe, J. Coll. Int. Sci., 159 (1993) 405.
28 C. H. Ruscher, Phys. Chem. Miner., 23 (1996) 50.
29 B. Champagnon, G. Panczer, C. Chemarin and B. Humbert-Labeaumaz, J. Non-Crystal. Solids, 196 (1996) 221.
30 N. Q. Liem, G. Sagon, V. X. Quang, H. V. Tan and P. Colomban, J. Raman Spect., 31 (2000) 933.
31 B. Humbert, A. Burneau, J. P. Gallas and J. C. Lavally, J. Non-Crystal. Solids, 143 (1992) 75.
32 H. J. Percival, J. Duncan and P. K. Foster, J. Amer. Ceram. Soc., 57 (1974) 57.
33 S. Shoval, Thermochim. Acta, 135 (1988) 243.